

Directional scattering of light by silicon nanoparticles and nanostructures due to high-order multipoles contribution

Pavel Terekhov^{1,2}

¹Ben-Gurion University

²ITMO University

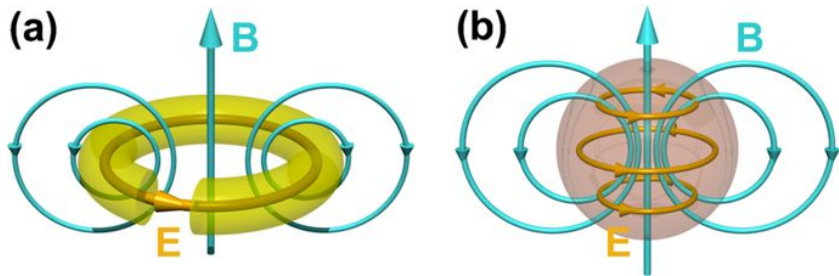
terekhovpd@gmail.com

October 16, 2018

Outline

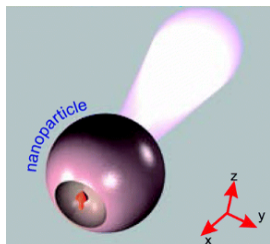
- 1 State of the Art
- 2 Multipole decomposition method
- 3 Resonant scattering of light by high refractive-index dielectric nanoparticles
 - Silicon cylinders
 - Summary on resonant forward scattering
 - Silicon cubes and pyramids
 - Influence of illumination direction
 - Summary on multipole excitations in Si nanoparticles
- 4 Influence of surrounding media refractive index
 - Multipole decomposition spectra in different media
 - Radiation patterns
 - Summary on influence of different media
- 5 Multipole analysis of periodic metasurfaces and engineering of broadband absorption
 - Multipole analysis of the cubical metasurfaces and the lattice invisibility effect
 - All-dielectric metasurfaces engineered absorption
 - Summary on dielectric metasurfaces research
- 6 Other projects of Light-on-a-Chip group

State-of-Art

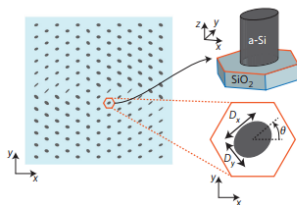


Schematic representation of electric and magnetic field distribution inside a metallic split-ring resonator (a) and a high-refractive index dielectric nanoparticle (b) at magnetic resonance wavelength.

State-of-Art

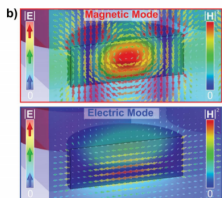
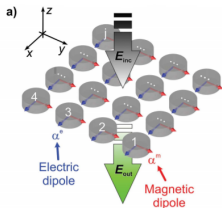


Krasnok A. E. et al. '**Superdirective dielectric nanoantennas.**' *Nanoscale* 6:13 (2012): 7354-7361

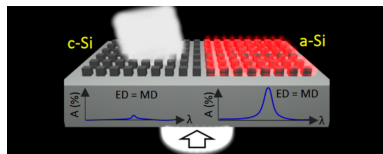


Arbabi A. et al. '**Dielectric metasurfaces for complete control of phase and polarization with subwavelength spatial resolution and high transmission.**' *Nature nanotechnology* 10 (2015): 937-942

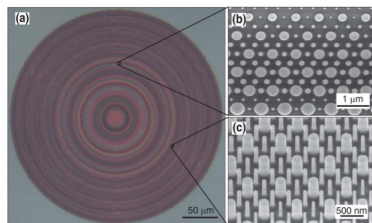
State-of-Art



Decker M. et al. 'High-Efficiency Dielectric Huygens Surfaces' *Advanced Optical Materials* 3.6 (2015): 813-820



Chi-Yin Yang et al. 'Nonradiating Silicon Nanoantenna Metasurfaces as Narrowband Absorbers.' *ACS Photonics* 5 (2018): 25962601



Arbabi E. et al. 'Multiwavelength polarization-insensitive lenses based on dielectric metasurfaces with meta-molecules.' *Optica* 3.6 (2016): 628-633

Multipole decomposition method

Regular electric dipole moment of the scatterer

$$\mathbf{p} = \int \mathbf{P}(\mathbf{r}') d\mathbf{r}'$$

Scattering cross-section (considering multipole moments up to the electric octupole moment)

$$\begin{aligned} \sigma_{\text{sca}} \simeq & \frac{k_0^4}{6\pi\epsilon_0^2|\mathbf{E}_{\text{inc}}|^2} |\mathbf{p} + \frac{ik_0\epsilon_d}{c} \mathbf{T}|^2 + \frac{k_0^4\epsilon_d\mu_0}{6\pi\epsilon_0|\mathbf{E}_{\text{inc}}|^2} |\mathbf{m}|^2 \\ & + \frac{k_0^6\epsilon_d}{720\pi\epsilon_0^2|\mathbf{E}_{\text{inc}}|^2} \sum |Q_{\alpha\beta}|^2 + \frac{k_0^6\epsilon_d^2\mu_0}{80\pi\epsilon_0|\mathbf{E}_{\text{inc}}|^2} \sum |M_{\alpha\beta}|^2 \\ & + \frac{k_0^8\epsilon_d^2}{1890\pi\epsilon_0^2|\mathbf{E}_{\text{inc}}|^2} \sum |O_{\alpha\beta\gamma}|^2. \end{aligned}$$

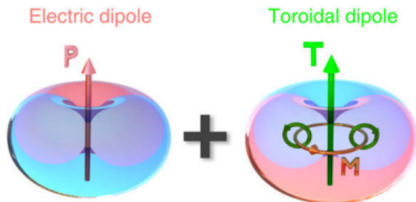
Toroidal dipole moment, having the same radiation pattern as ED

$$\mathbf{T} = \frac{i\omega}{10} \int \{2\mathbf{r}'^2 \mathbf{P}(\mathbf{r}') - (\mathbf{r}' \cdot \mathbf{P}(\mathbf{r}')) \mathbf{r}'\} d\mathbf{r}'$$

Miroshnichenko A. E. et al., Nature communications 6 (2015): 8069

Evlyukhin A. B. et al., Physical Review B. 94.20 (2016): 205434

Toroidal dipole moment



In the terms of irreducible representation of Cartesian multipoles toroidal dipole moment is a term which is separated from symmetrized and traceless magnetic quadrupole and electric octupole moments. It has the same far-field radiation pattern as electric dipole moment and can interfere with it constructively and destructively.

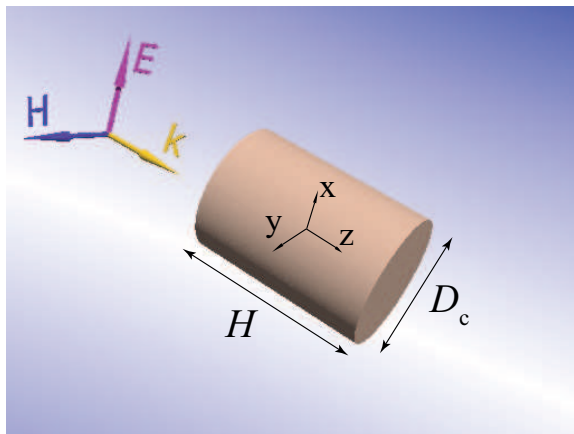
Resonant scattering of light by high refractive-index dielectric nanoparticles



Terekhov P.D. et al., 'Resonant forward scattering of light by high-refractive-index dielectric nanoparticles with toroidal dipole contribution', *Optics Letters* 42:4. 835-838 (2017).

Terekhov P.D. et al., 'Multipolar response of non-spherical silicon nanoparticles in the visible and near-infrared spectral ranges', *Physical Review B* 96, 035443 (2017)

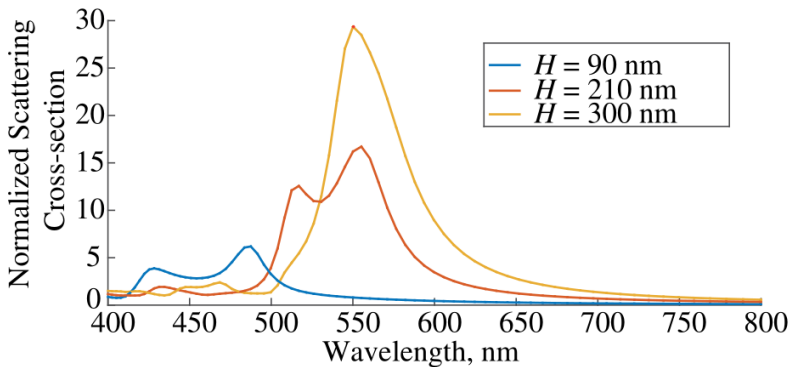
System



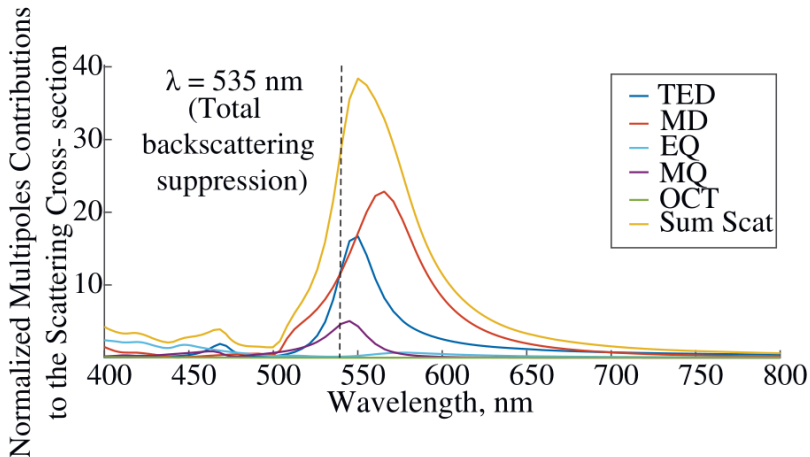
$$H = 90 - 300 \text{ nm}, D_c = 100 \text{ nm}.$$

$$\lambda = 400 - 800 \text{ nm}.$$

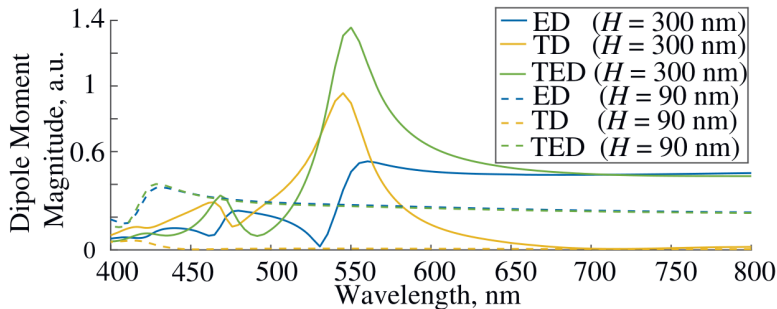
Scattering cross-section of nanocylinders with different H



Multipole contributions to the scattering cross-section

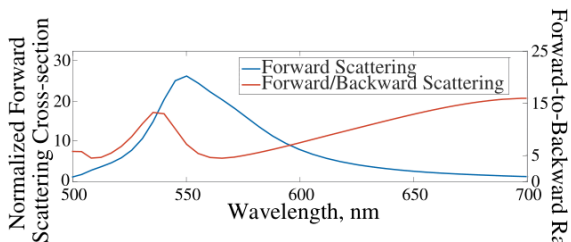


Spectra of the absolute values of TED, ED, and TD



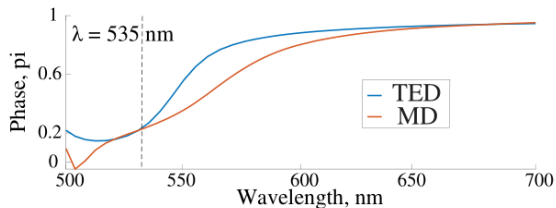
$H = 90$ and 300 nm, $D_c = 100$ nm.

Forward/Backward Scattering and TED & MD Phases

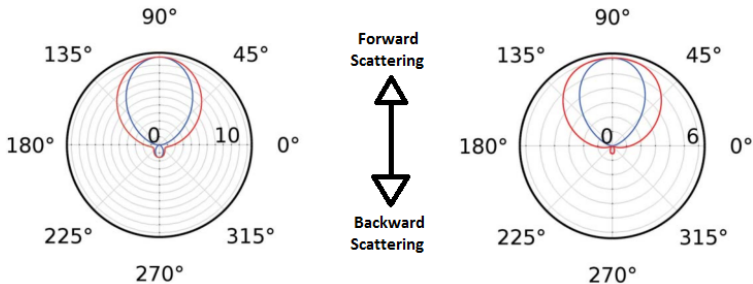


$$H = 300 \text{ nm}$$

$$D_c = 100 \text{ nm}$$



Radiation Patterns



Radiation pattern at the maximum scattering wavelength

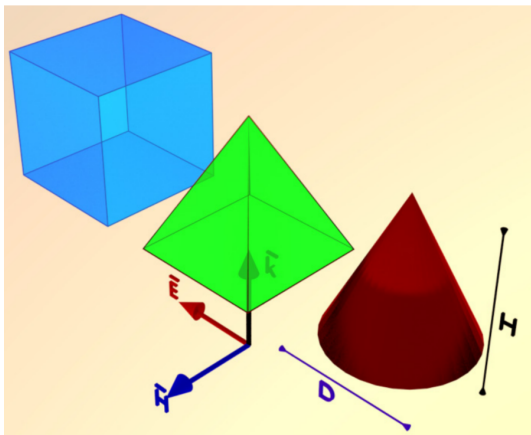
Radiation pattern at the maximum forward/backward scattering wavelength (**Kerker effect**)

Cylindrical nanoparticle, $H = 300$ nm, $D_c = 100$ nm.

Summary on resonant forward scattering

- Constructive interference between toroidal and electric dipole moments of the nanoparticle can be realized in silicon nanoparticles
- Total electric dipole moment with dominant contribution of the toroidal dipole is resonantly excited in the nanoparticles and so called super-dipole mode is numerically demonstrated
- Due to the interference between electromagnetic fields generated by the total electric dipole and magnetic dipole moments of the nanoparticles, the Kerker-type effect (backward scattering suppression) can be numerically shown

Nanoparticles of a different shape

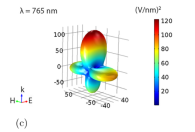
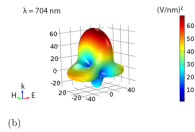
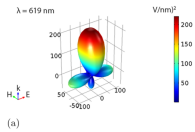
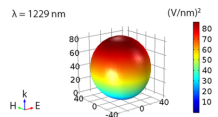
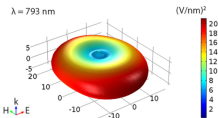
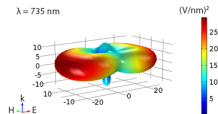
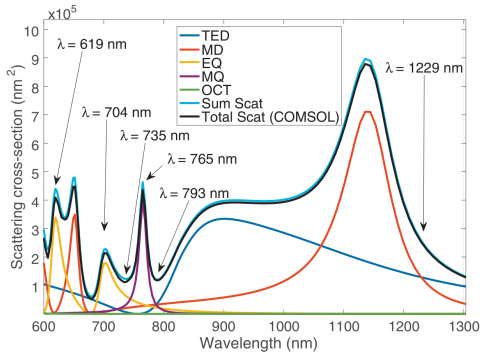


Parallelepiped, pyramid, and cone with varying height H and diameter of $D = 250$ nm.

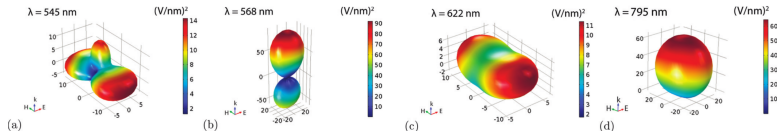
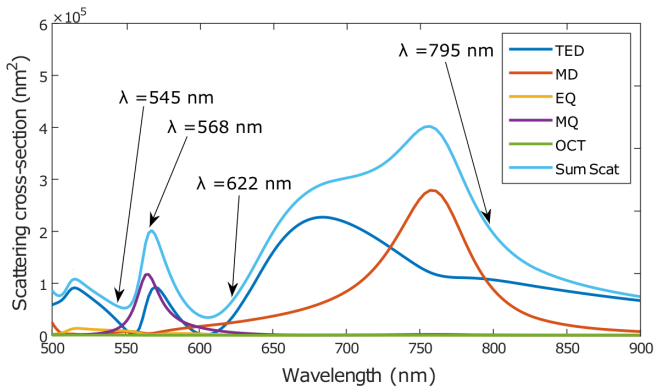
↳ Resonant scattering of light by high refractive-index dielectric nanoparticles

↳ Silicon cubes and pyramids

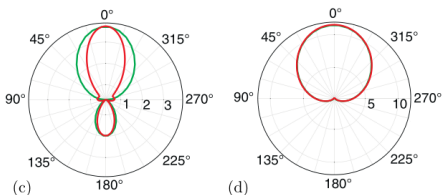
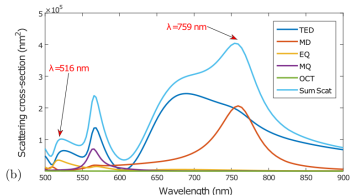
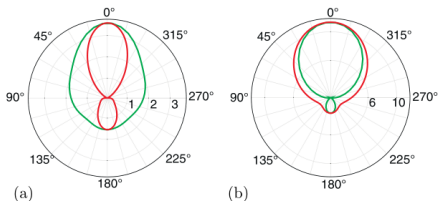
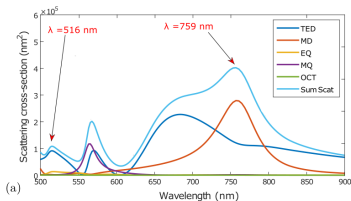
Multipole contributions to the scattering cross-section



Multipole Decomposition of SCS of nanopyramid



Nonsymmetry effect in nanopyramid scattering



2D scattering patterns: the incidence (a,b) from the pyramid base, $\lambda = 516 \text{ nm}$ and 759 nm , ((c,d) from the pyramid top, $\lambda = 516 \text{ nm}$ and 759 nm . Red (green) contour corresponds to the plane of the incident E (H) polarization.

Summary on multipole excitations in Si nanoparticles

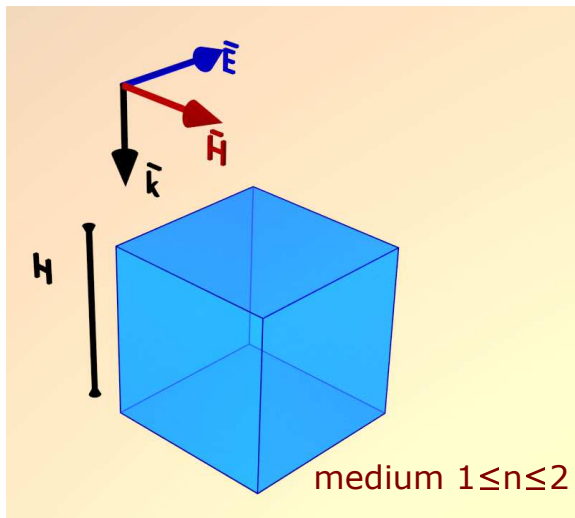
- Multipoles up to the third order that were excited by light in cubical and pyramidal silicon nanoparticles were investigated.
- Peculiar scattering patterns (even side-scattering) with certain predominant scattering directions can be obtained by tuning the spectral overlap of several multipoles.
- We showed that the effect of the asymmetrical multipole response in pyramidal particles depends on the illumination direction.
- Our investigation provides important information about the roles of the high order multipoles in the light scattering by nonspherical nanoparticles and can be applied for the development of the nanoantennas, metasurfaces, coatings etc.

Influence of surrounding media refractive index



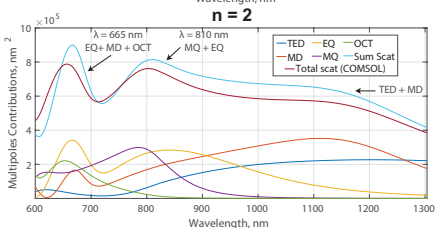
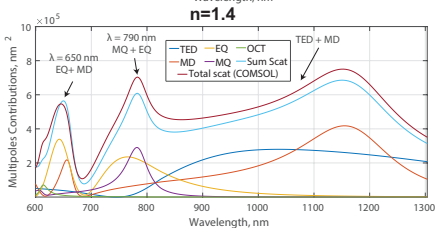
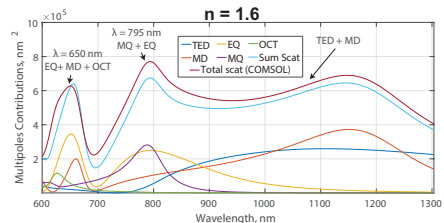
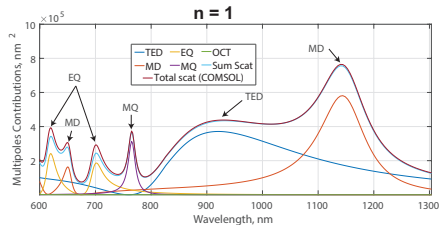
Terekhov P.D. et al., 'Strong asymmetry of a forward scattered light by a silicon nanocube immersed in a dense refractive index media' (*In preparation*)

System schematics



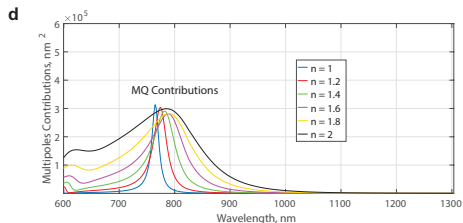
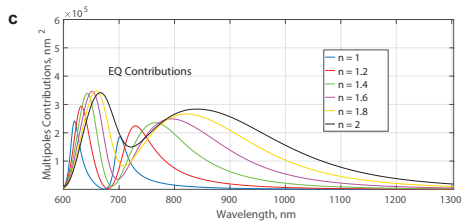
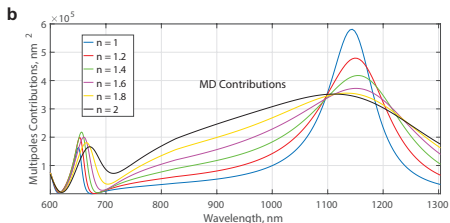
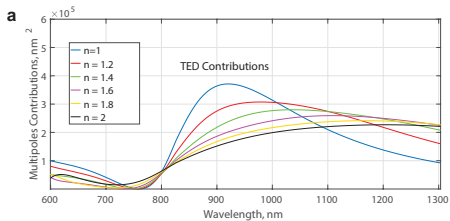
- ↳ Influence of surrounding media refractive index
- ↳ Multipole decomposition spectra in different media

Multipole decomposition of scattering cross-section

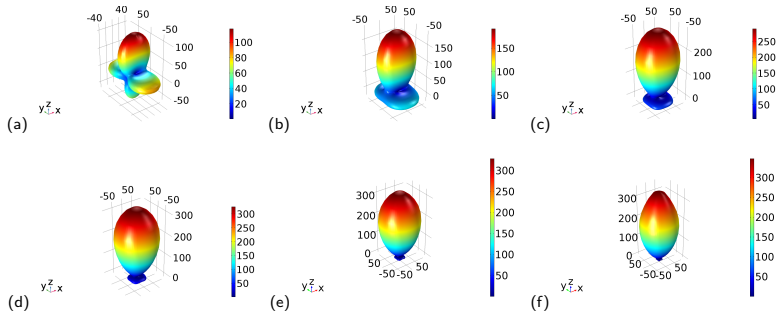


- └ Influence of surrounding media refractive index
- └ Multipole decomposition spectra in different media

Evolution of multipole moments as n changes

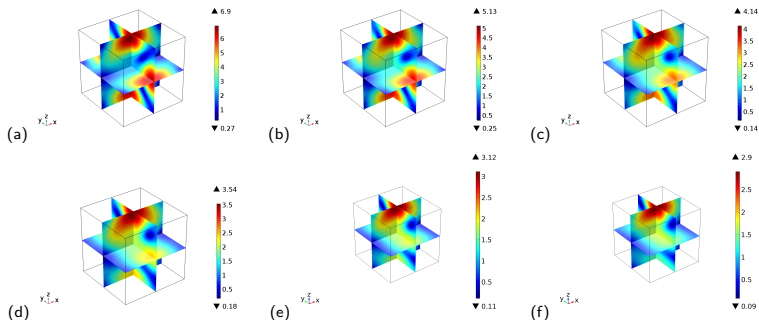


3D radiation patterns in the area of MQ resonance



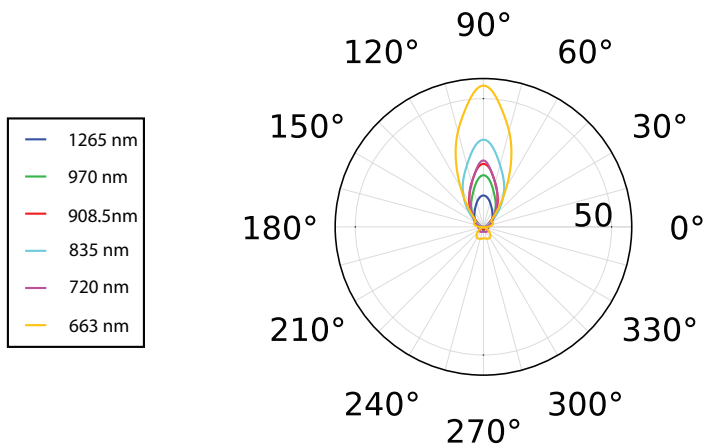
Radiation patterns for (a) $n_{env} = 1, \lambda = 765nm$ (b) $n_{env} = 1.2, \lambda = 775nm$
 (c) $n_{env} = 1.4, \lambda = 783nm$ (d) $n_{env} = 1.6, \lambda = 789nm$ (e) $n_{env} = 1.8, \lambda = 789nm$
 (f) $n_{env} = 2, \lambda = 789nm$.

3D current distributions in the area of MQ resonance



Electric field distribution inside the nanocube for (a) $n_{env} = 1$, $\lambda = 765nm$ (b) $n_{env} = 1.2$, $\lambda = 775nm$ (c) $n_{env} = 1.4$, $\lambda = 783nm$ (d) $n_{env} = 1.6$, $\lambda = 789nm$ (e) $n_{env} = 1.8$, $\lambda = 789nm$ (f) $n_{env} = 2$, $\lambda = 789nm$.

2D radiation patterns in $n = 2$ media for several λ



2D radiation patterns in $n = 2$ media for λ mentioned in the legend.

Conclusions

- Directly calculated scattering cross-sections are close to the sum of multipole contributions, but there is some difference for high-index surroundings.
- Electric multipole moments (TED, EQ) experience stronger red-shift than magnetic multipole moments (MD, MQ).
- Separated scattering cross-section peaks transform to smoother merged peaks as n rises; separated MQ and EQ resonances do not longer exist for high-index media.
- For high-index media the broadband forward scattering amplification takes place.
- Electric field inside the nanocube concentrates in the forward part of the particle as n rises.

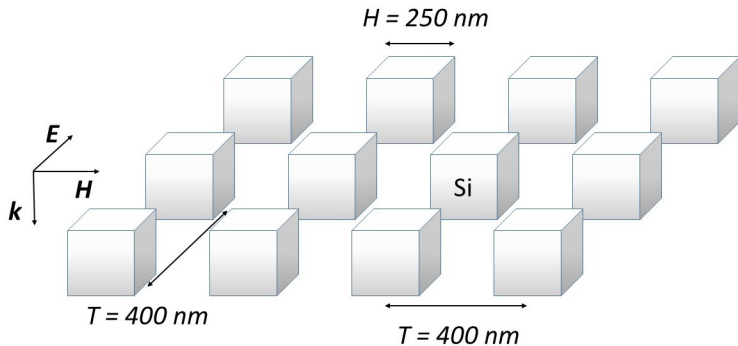
Multipole analysis of periodic metasurfaces and engineering of broadband absorption



Terekhov P.D. et al., 'Multipole analysis of dielectric metasurfaces and lattice invisibility effect' (Submitted to *Physical Review B*)

Terekhov P.D. et al., 'Enhanced absorption in all-dielectric metasurfaces due to magnetic dipole excitation.' (Submitted to *Nature Scientific Reports*)

Considered System



Multipole analysis of periodic arrays

In dipole approximation, the electric field reflection r and transmission t coefficients of rectangular 2D infinite arrays are

$$r = \frac{ik_d}{E_0 2S_L \epsilon_0 \epsilon_d} \left[p_x - \frac{1}{v_d} m_y \right],$$

$$t = 1 + \frac{ik_d}{E_0 2S_L \epsilon_0 \epsilon_d} \left[p_x + \frac{1}{v_d} m_y \right].$$

The scattered electric field \mathbf{E}^{sc} obtained for a single nanoparticle

$$\begin{aligned} \mathbf{E}^{\text{sc}}(\mathbf{n}) \sim & \left([\mathbf{n} \times [\mathbf{p} \times \mathbf{n}]] + \frac{1}{v_d} [\mathbf{m} \times \mathbf{n}] + \frac{ik_d}{6} [\mathbf{n} \times [\mathbf{n} \times \hat{Q}\mathbf{n}]] \right. \\ & \left. + \frac{ik_d}{2v_d} [\mathbf{n} \times (\hat{M}\mathbf{n})] + \frac{k_d^2}{6} [\mathbf{n} \times [\mathbf{n} \times \hat{O}(\mathbf{n}\mathbf{n})]] \right). \end{aligned}$$

Evlyukhin A. B. et al., *Physical Review B* 82, 045404 (2010)

Evlyukhin A. B. et al., *Physical Review B*. 94.20 (2016): 205434

Terekhov P. D. et al., *Physical Review B*. (under review)

Multipole analysis of periodic arrays

For the forward scattering $\mathbf{n} = (0, 0, 1)$, and the backward scattering $\mathbf{n} = (0, 0, -1)$. Inserting $\mathbf{n} = (0, 0, n_z)$ in the previous expression we obtain for the case of the x-polarization

$$E_x^{\text{sc}} \sim \left(p_x n_z^2 + \frac{1}{v_d} m_y n_z - \frac{ik_d}{6} Q_{xz} n_z^3 - \frac{ik_d}{2v_d} M_{yz} n_z^2 - \frac{k_d^2}{6} O_{xzz} n_z^4 \right),$$

After some derivations, by the replacing the expressions in the brackets by the multipole decompositions of the single particle scattering amplitude (*which is our straightforward conclusion*) we obtain

$$r = \frac{ik_d}{E_0 2S_L \epsilon_0 \epsilon_d} \left(p_x - \frac{1}{v_d} m_y + \frac{ik_d}{6} Q_{xz} - \frac{ik_d}{2v_d} M_{yz} - \frac{k_d^2}{6} O_{xzz} \right),$$

$$t = 1 + \frac{ik_d}{E_0 2S_L \epsilon_0 \epsilon_d} \left(p_x + \frac{1}{v_d} m_y - \frac{ik_d}{6} Q_{xz} - \frac{ik_d}{2v_d} M_{yz} - \frac{k_d^2}{6} O_{xzz} \right).$$

Multipole analysis of periodic arrays

The reflection and transmission coefficients are

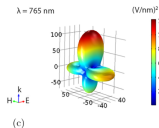
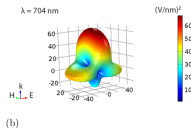
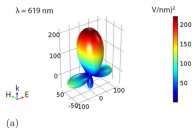
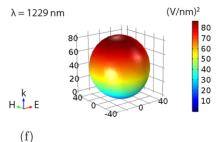
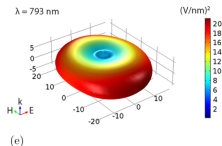
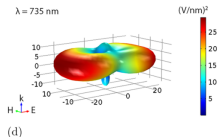
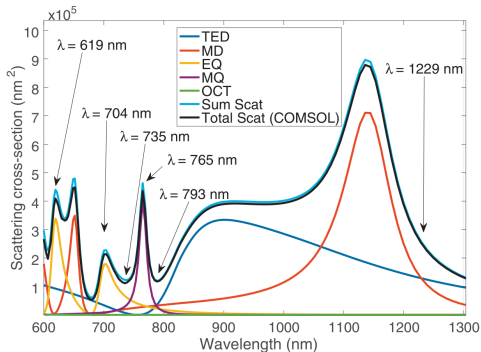
$$R = |r|^2, \quad T = |t|^2.$$

Then the absorption coefficient A could be derived from the following expression $A = 1 - R - T$.

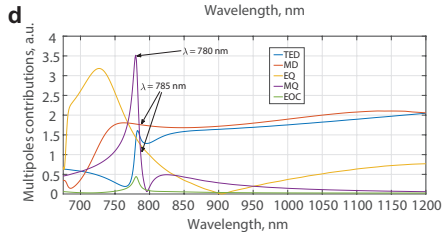
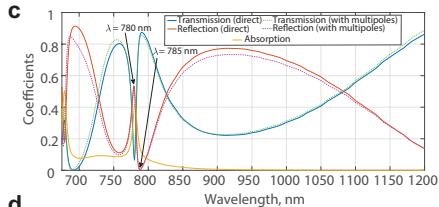
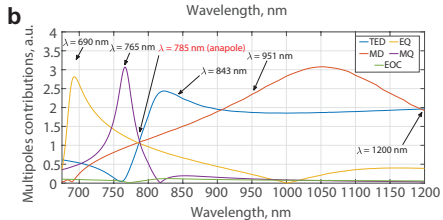
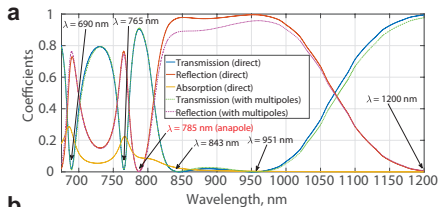
By developing this technique we revealed how the analytical multipole decompositions of field reflection and transmission coefficients of nanoparticle arrays can be obtained from the single particle scattering. Such multipole analysis allows to explain the origins of the reflection and transmission features.

Terekhov P. D. et al., *Physical Review B*. (under review)

Multipole contributions to the scattering cross-section

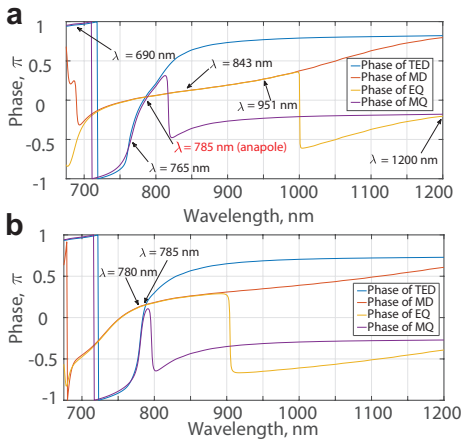


Periodic silicon structure in air



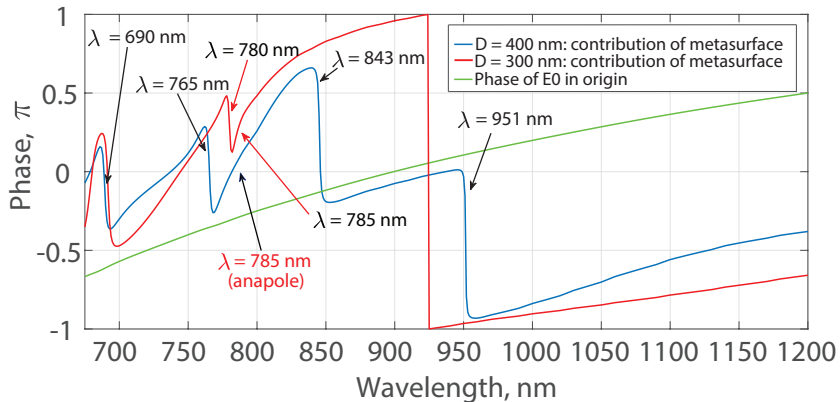
(a,b) $D = 400$ nm (c,d) $D = 300$ nm

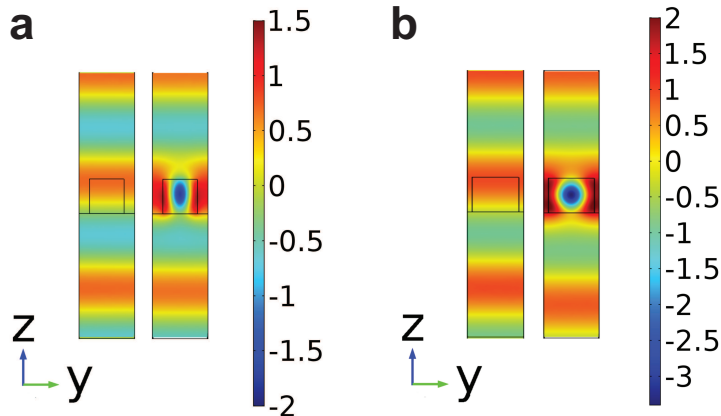
Multipole phases



Multipole contribution phases for (a) $D = 400$ nm (b) $D = 300$ nm

Transmitted Electric field phases

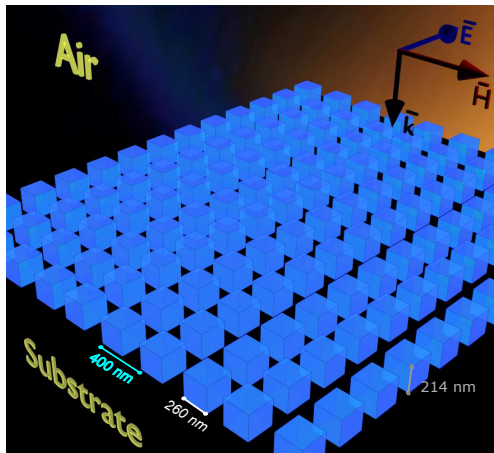


Field cross-section for $D = 400$ nm and $D = 300$ nm

└ Multipole analysis of periodic metasurfaces and engineering of broadband absorption

└ All-dielectric metasurfaces engineered absorption

System

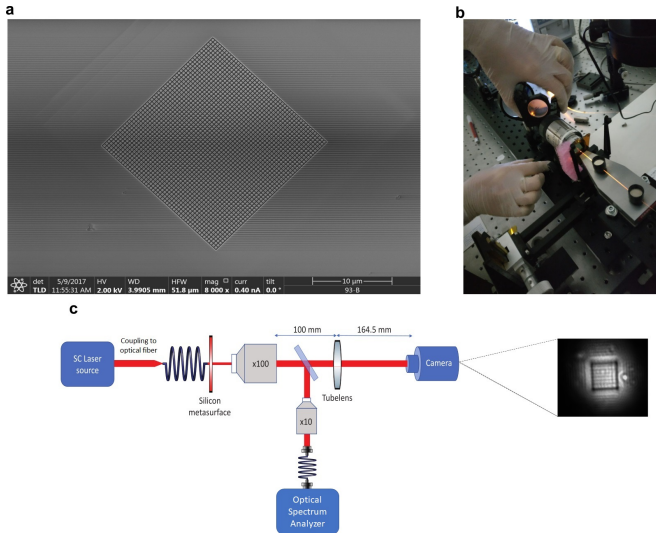


Artistic image of the fabricated metasurface.

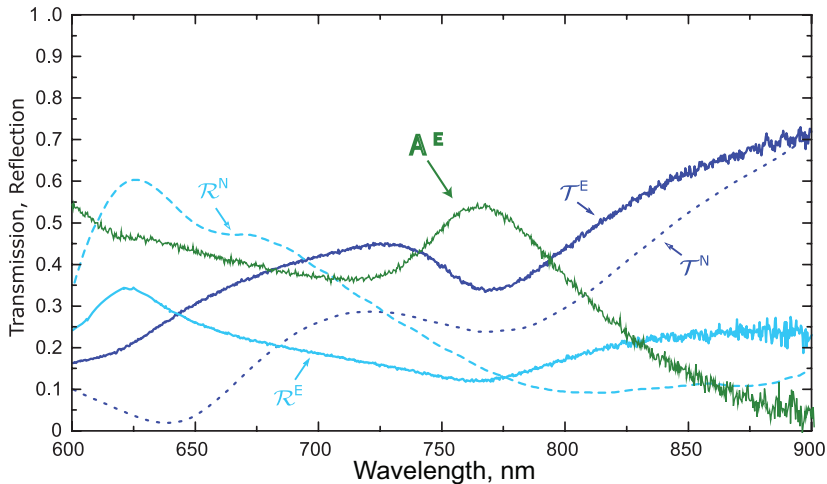
└ Multipole analysis of periodic metasurfaces and engineering of broadband absorption

└ All-dielectric metasurfaces engineered absorption

Proof of concept of experiment



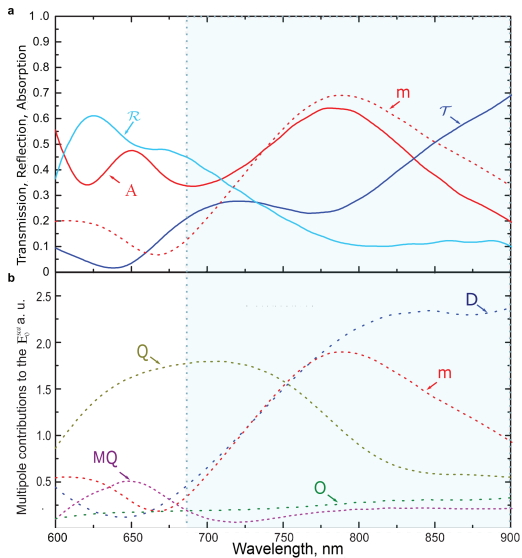
Experiment - Modelling comparison of coefficients



- ↳ Multipole analysis of periodic metasurfaces and engineering of broadband absorption

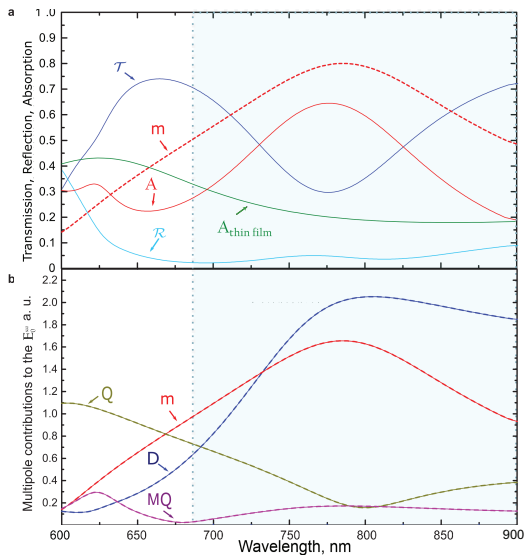
- ↳ All-dielectric metasurfaces engineered absorption

Multipole analysis of the metasurface on the substrate



According to multipole decomposition, the presented reflection peak corresponds to the area of predominating EQ resonance, and the dip in transmission can be associated with the absorption peak; this peak can be associated with MD and TED resonances excitation. Multipole decomposition has been performed using the similar method as for single nanoparticle in the air.

Multipole analysis of the metasurface in air



The absorption peak remains in the same region for the case of air surrounding. It proves that the considered effect does not depend on the substrate influence.

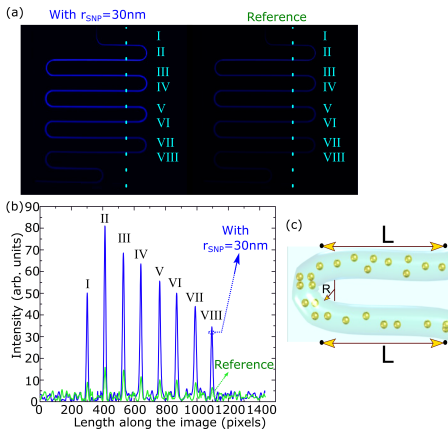
Summary on dielectric metasurfaces research

- Silicon metasurface based on single particle investigations have been studied.
- Multipole analysis of the periodic arrays of particles has been implemented.
- Multipoles contribution to electric field amplitudes was compared for 1) single cube and 2) array of cubes.
- The lattice invisibility effect was demonstrated for the c-Si metasurface in air
- a-Si metasurfaces on bk7 substrate have been investigated numerically and experimentally.
- EQ and MD resonance areas are associated with the reflection and absorption peaks correspondingly.

Other projects of Light-on-a-Chip group

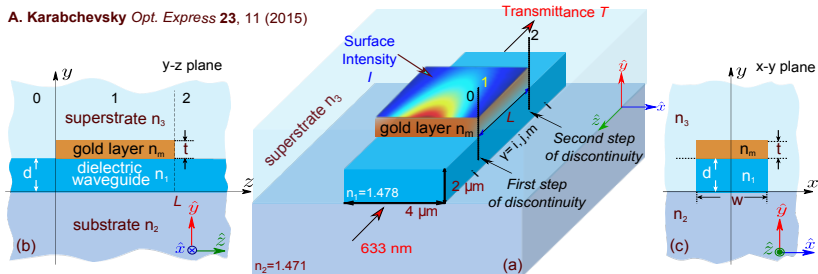


Plasmonic nanoantennas



Chemiluminescence enhancement in microfluidic system.

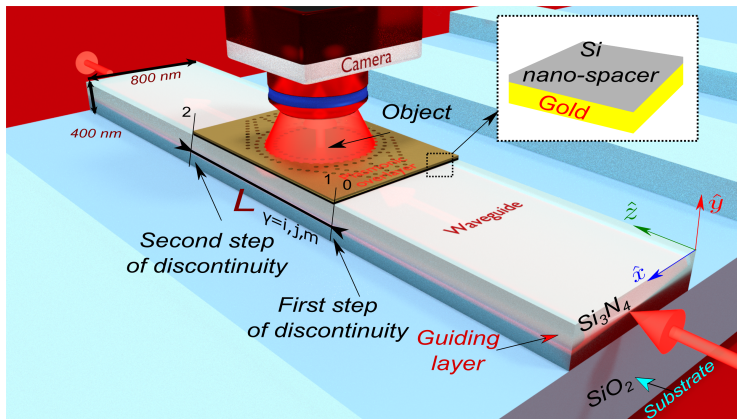
Plasmonic structures



(a) 3D schematic of composite plasmonic doped SiO_2 waveguide; cross-sections (b) (y - z) plane and (c) (x - y) plane (dimensions are shown out of scale).

$$n_m = 0.197 - j3.466, n_3 = 1.3 : 1.44 \text{ RIU}$$

Hiding above the carpet



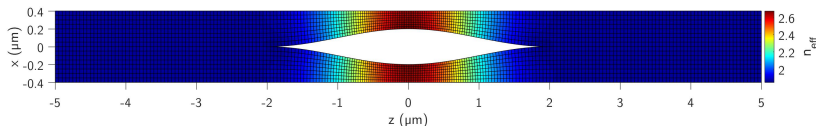
Composite plasmonic waveguide cloak design

If the mapping satisfies the CauchyRiemann conditions given by

$$\partial x' / \partial x = \partial z' / \partial z,$$

$$\partial x' / \partial z = -\partial z' / \partial x,$$

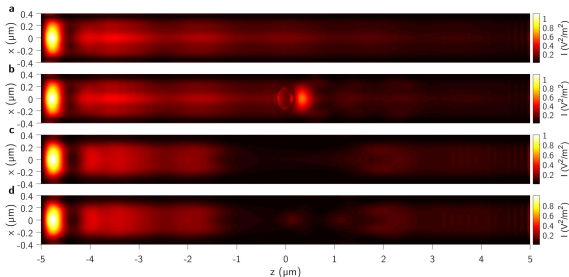
the transformed material becomes inhomogeneous and isotropic. The resulting transformation is composed of a quasi-orthogonal grid with an effective index in each cell:



Transformed mesh using quasi-conformal transformation theme (black mesh) and calculated effective mode index, n_{eff} .

Cloaking results and performance

The figure below shows calculated integrated total surface intensity to assess the effectiveness of evanescent invisibility cloak with a composite plasmonic waveguide.



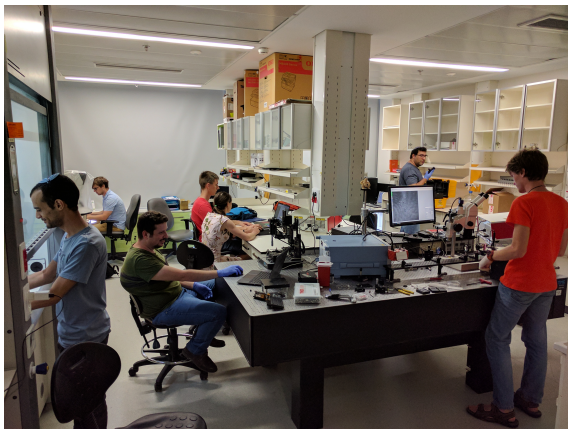
Calculated spatial surface intensities $|\mathcal{E}_y(x, z)|^2$ at $y = y_s$ in the composite plasmonic waveguide: (a) with slab gold overlayer, (b) with slab gold overlayer an object index of 1.3, (c) with transformed metasurface and (d) with transformed metasurface and an object.

Our works

My relevant publications:

- 1 Terekhov P. D.** et al. 'Resonant forward scattering of light by high-refractive-index dielectric nanoparticles with toroidal dipole contribution', *Optics Letters* 42:4. 835-838 (2017).
- 2 Terekhov P. D.** et al. 'Multipolar response of non-spherical silicon nanoparticles in the visible and near-infrared spectral ranges', *Physical Review B* 96, 035443 (2017).
- 3 Terekhov P.D.** et al., 'Strong asymmetry of a forward scattered light by a silicon nanocube immersed in a dense refractive index media' *In preparation*
- 4 Terekhov P.D.** et al., 'Multipole analysis of dielectric metasurfaces and lattice invisibility effect', *Submitted to Physical Review B*
- 5 Terekhov P.D.** et al., 'All-dielectric metasurfaces engineered absorption', *Submitted to Nature Scientific Reports*

Our Team



Our team in Ben-Gurion University of Negev.
Thanks for your attention!

Multipoles' expressions

$$\mathbf{p} = \int \mathbf{P}(\mathbf{r}') d\mathbf{r}' \quad (2)$$

$$\mathbf{m} = -\frac{i\omega}{2} \int [\mathbf{r}' \times \mathbf{P}(\mathbf{r}')] d\mathbf{r}' \quad (3)$$

$$\mathbf{T} = \frac{i\omega}{10} \int \{2\mathbf{r}'^2 \mathbf{P}(\mathbf{r}') - (\mathbf{r}' \cdot \mathbf{P}(\mathbf{r}')) \mathbf{r}'\} d\mathbf{r}' \quad (4)$$

$$Q = 3 \int [\mathbf{r}' \mathbf{P}(\mathbf{r}') + \mathbf{P}(\mathbf{r}') \mathbf{r}' - \frac{2}{3} (\mathbf{r}' \cdot \mathbf{P}(\mathbf{r}')) \hat{U}] d\mathbf{r}' \quad (5)$$

$$M = \frac{\omega}{3i} \int \{[\mathbf{r}' \times \mathbf{P}(\mathbf{r}')] \mathbf{r}' + \mathbf{r}' [\mathbf{r}' \times \mathbf{P}(\mathbf{r}')]\} d\mathbf{r}' \quad (6)$$